

# RSC Advances

Accepted Manuscript



This is an Accepted Manuscript, which has been through the Royal Society of Chemistry peer review process and has been accepted for publication.

Accepted Manuscripts are published online shortly after acceptance, before technical editing, formatting and proof reading. Using this free service, authors can make their results available to the community, in citable form, before we publish the edited article. We will replace this Accepted Manuscript with the edited and formatted Advance Article as soon as it is available.

You can find more information about Accepted Manuscripts in the [author guidelines](#).

Please note that technical editing may introduce minor changes to the text and/or graphics, which may alter content. The journal's standard [Terms & Conditions](#) and the ethical guidelines, outlined in our [author and reviewer resource centre](#), still apply. In no event shall the Royal Society of Chemistry be held responsible for any errors or omissions in this Accepted Manuscript or any consequences arising from the use of any information it contains.

**Microwave assisted synthesis of carbon dots-zinc  
oxide/multi-walled carbon nanotubes and its application in  
electrochemical sensor for simultaneous detection of hydroquinone  
and catechol**

Yaru Yan<sup>a,†</sup>, Qitong Huang<sup>b,c,†</sup>, Chan Wei<sup>a,†</sup>, Shirong Hu<sup>a,\*</sup>, Hanqiang Zhang<sup>a</sup>, Wuxiang Zhang<sup>a</sup>,  
Weize Yang<sup>a</sup>, Peihui Dong<sup>a</sup>, Menglin Zhu<sup>a</sup>, Zhaoming Wang<sup>a</sup>

<sup>a</sup> College of Chemistry and Environment, Minnan Normal University,

Zhangzhou 363000, P.R. China

<sup>b</sup> Department of Food and Biological Engineering, Zhanzhou Institute of Technology,

Zhangzhou 363000, P.R. China

<sup>c</sup> The application technology of collaborative innovation center for Fine Chemicals in Fujian

Province, Zhangzhou 363000, P.R. China

<sup>†</sup> These authors contributed equally to this work.

---

\* Corresponding author: Tel.: +86 596 2528075. Fax: +86 596 2528075

E-mail address: Hushirong6666@163.com (prof. S. Hu).

**Abstract** A facile, efficient and rapid microwave assisted method was developed to compound the carbon dots-zinc oxide/multi-walled carbon nanotubes (CDs-ZnO/MWCNTs) composite. And the CDs-ZnO/MWCNTs material was characterized by scanning electron microscope (SEM), high-resolution transmission electron microscopy (HRTEM), Fourier transform infrared spectroscopy (FT-IR) and X-ray diffraction (XRD). The electrode modified with CDs-ZnO/MWCNTs composite was applied for simultaneous determination of hydroquinone (HQ) and catechol (CC) in 0.1 M phosphate buffer solutions (PBS, pH = 4.5). The anodic potential difference ( $\Delta E_{pa}$ ) between HQ and CC was 104 mV, which indicated the modified electrode could detect the HQ and CC simultaneously. The calibration curves of HQ and CC were obtained both in the range of 5.0 to 200  $\mu\text{M}$  with the detection limits (S/N=3) of 0.02  $\mu\text{M}$  and 0.04  $\mu\text{M}$  respectively. The modified electrode was applied to detect HQ and CC in the tap water and the rate of recoveries were 99.3% - 105.4% of HQ and 104.3% - 110.1% of CC.

**Keywords** Electrochemical sensor; Carbon dots; Hydroquinone; Catechol; Microwave assisted synthesis; Simultaneous determination.

## 1. Introduction

Hydroquinone (HQ) and catechol (CC) have been widely used in tanning, dye, chemical, photostabilizer, pesticides and some other fields closing to our life.<sup>1,2</sup> However, they also widely exist in environment as a kind of important environmental pollutant by the US Environmental Protection Agency (EPA) and the European Union (EU) because of their high toxicity and difficult degradation in the ecological system.<sup>3</sup> They can enter human's body to erode the skin and mucosa, and even the inhibit nerve center system.<sup>4,5</sup> Nowadays many methods have been used to detect HQ and CC simultaneously, for example, gas chromatography/mass spectrometry<sup>6,7</sup>, high performance liquid chromatography<sup>8,9</sup>, synchronous fluorescence<sup>10</sup> and electrochemical methods<sup>11,12</sup>. The equipment of chromatography is expensive and the operation is trivial. The accuracy of synchronous fluorescence needs improving. Electrochemical methods have drawn scientists' attention with the reasons of fast response, low cost, high sensitivity and selectivity in recent years.<sup>1,13,14</sup> However, it is a challenge to determinate HQ and CC simultaneously due to their similar structures, physicochemical properties and coexistence in environmental samples<sup>15,16</sup>. Because their redox peaks usually present overlapped that they can't be distinguished at conventional electrodes such as glassy carbon electrode (GCE).<sup>15,17</sup> It is urgent need to develop the innovative modified electrode with catalytic activity and good conductivity.

As a kind of one-dimensional (1D) material, multi-walled carbon nanotubes (MWCNTs) can be thought as several concentric tubes of graphene fitted one inside the other.<sup>18,19</sup> Owing to their high electronic conductivity, good mechanical properties and interesting electrocatalytic compatibility with electroactive varieties, MWCNTs have been applied in electrochemistry for a long time.<sup>18,20</sup> MWCNTs can improve the electrochemical performance by the way of promoting the electron

transfer reactions of various molecules and increasing the electroactive surface area of the modified electrode.<sup>21,22</sup> The sensors based on MWCNTs were successfully applied to distinguish ranges of significant analytes such as urea and other important electroactive species.<sup>23, 24</sup> However, the pristine MWCNTs are insoluble in routine solvents due to the intrinsic van der Waals interactions between the carbon tubes.<sup>25,26</sup> Therefore, MWCNTs have to be modified before connecting with others materials. In this work, we used a conventional methods to acidate MWCNTs with the mixed acid of H<sub>2</sub>SO<sub>4</sub> and HNO<sub>3</sub> (V/V=3:1).<sup>27,28</sup> As another carbon material, carbon dots (CDs) have attracted extensive attention owing to their small sizes, excellent water solubility, biocompatibility, photostability and nontoxicity.<sup>29-31</sup> There are lots of carboxyl groups at CDs' surface which can easier connect to other materials and enhance the redox response of HQ and CC. There are little literatures about CDs in electrochemistry field.<sup>32</sup> It is a challenge to develop the electrochemical sensors based on CDs.

At present various nano-metallic oxide materials have been applied in electrochemistry. ZnO nanostructures, as a kind of semiconductor material, play an important role in material synthesis due to their unique properties such as nontoxic nature, high chemical stability, high-electron communication features, electrochemical activities, and good piezoelectric properties.<sup>23,33</sup> There are many different morphologies of ZnO nanostructures such as nanowire<sup>34</sup>, nanotubes<sup>35</sup> and nanoparticles<sup>36</sup>. In this work, we synthesized ZnO particles because the nano-particles easier to link with CDs and MWCNTs from space.

Herein, we developed a facile, efficient and convenient microwave synthesis method to fabricate the CDs-ZnO/MWCNTs composite. The FT-IR data confirmed the synthesis route of CDs-ZnO/MWCNTs. Due to the unique properties that mentioned above of CDs, ZnO and

MWCNTs, the modified CDs-ZnO/MWCNTs electrode could enhance the electrochemical performance for simultaneous detection of HQ and CC obviously. The electrochemical properties of CDs-ZnO/MWCNTs/GCE were characterized by cyclic voltammetry (CV) and differential pulse voltammetry (DPV). The peak current was linear with the concentration of HQ and CC respectively, and the proposed sensor was applied to successfully detect the HQ and CC in real tap water sample.

## 2. Experimental

### 2.1 Chemical reagents and instrumentation

HQ was brought from DA hao fine chemicals Co., LTD (Shantou, Guangdong, China) and CC was purchased from Sinopharm Chemical Reagent Shanghai Co., Ltd (China). MWCNTs were brought from Shenzhen Nanotech Port Co., Ltd. Anhydrous ethanol, nitric acid, sulfuric acid, glucose, polyethylene glycol-200 (PEG-200) and zinc nitrate hexahydrate ( $\text{Zn}(\text{NO}_3)_2 \cdot 6\text{H}_2\text{O}$ ) were purchased from Xilong Chemical Co., Ltd (Guangdong, china). Phosphate buffer solutions (PBS) (pH = 4.5) were obtained by mixing stock standard solutions of  $\text{Na}_2\text{HPO}_4 \cdot 12\text{H}_2\text{O}$  ( $0.1 \text{ mol L}^{-1}$ ),  $\text{NaH}_2\text{PO}_4 \cdot 2\text{H}_2\text{O}$  ( $0.1 \text{ mol L}^{-1}$ ) and KCl ( $1 \text{ m mol L}^{-1}$ ). And the perfluorinated resin solution (Nafion) was brought from Sigma-aldrich, Co., (USA). All solution was prepared by using ultrapure water.

The MWCNTs was acidized with the help of WH-200 ultrasonic cleaning machine. Monowave 300 (Anton Pear GmbH, Austria) was used for microwave irradiation synthesis of CDs and CDs-ZnO/MWCNTs. Vacuum rotary evaporation instrument (Guangzhou IKA laboratory technology Co., LTD) was used to remove the water in CDs solution. Fourier transform infrared spectroscopy (FT-IR) was obtained by using Thermo NICOLET iS 10 (Thermo Fisher Scientific,

America). Both cyclic voltammetry (CV) and differential pulse voltammetry (DPV) were obtained using CHI 660E electrochemical workstation (Shanghai Chen Hua Instruments Co., China) with a three-electrode system. All electrochemical experiments were conducted in 10 mL 0.1 M PBS (pH = 4.5) at room temperature. AE240 electronic analytical balance (Shanghai Mettler-Toledo Instruments Co., Ltd) was used for accurate weighing.

## 2.2 Synthesis of CDs-ZnO/MWCNTs

The CDs were prepared by microwave method with the help of Monowave 300. Firstly, 2.0000 g glucose was dissolved in 3 mL ultrapure water by ultrasound, followed by addition of 10.00 mL PEG-200. Secondly, the mixture was put into Monowave 300 and heated at 180 °C for 3 min to obtain a brownish red solution. Thirdly, the solution was dialyzed for 24 h using 1000 cutoffs dialysis membranes. Since the size of ZnO was affected by the composition of ethanol/water, the CDs aqueous solution was concentrated with the help of vacuum rotary evaporation. The solid product was dissolved with 60 mL anhydrous ethanol. Finally, the CDs ethanol solution was stored at 4 °C ready for future use. The MWCNTs were acidized by means of reflux in the mixed solution of sulfuric acid and nitric acid (v/v, 3:1) at 140 °C for 2 h.<sup>8</sup> Then the product was diluted and filtered with a cellulose membrane filter (pore size 0.25 μm) and washed with distilled water several times until the pH close to 7. The acidized MWCNTs was filtrated and dried in 100 °C.

0.25 M zinc nitrate hexahydrate ( $\text{Zn}(\text{NO}_3)_2 \cdot 6\text{H}_2\text{O}$ ) and 0.0500 g acidized MWCNTs were put into 30 mL glass vial (G30) before adding the 10 mL CDs ethanol solution in, and then dispersed by ultrasound. The mixture was put in Monowave 300 and heated for 3 min at 180 °C and the sediment was obtained. The product was washed with water and anhydrous ethanol several times in order to remove the impurity. Then purified product was dried at 100 °C in air dry oven and the

CDs-ZnO/MWCNTs composite was obtained. The possible mechanism was  $-\text{COOH}$  of CDs and MWCNTs had been formed the  $-\text{COOZnOH}$  when they were interacted with ZnO.

### 2.3 Electrode preparation

The bare glassy carbon electrode (GCE) was polished with 1.0  $\mu\text{m}$ , 0.3  $\mu\text{m}$ , 0.05  $\mu\text{m}$  alumina powder sequentially, then washed with distill water, ethanol and distill water successively in an ultrasonic bath, followed by blow with nitrogen.

0.0050 mg CDs-ZnO/MWCNTs composite was dispersed into 2 mL ultrapure water and then put in WH-200 ultrasonic cleaning machine to gain the CDs-ZnO/MWCNTs solution. 5  $\mu\text{L}$  of the CDs-ZnO/MWCNTs composite solution was dropped on GCE surface. After the modified electrode dried in air, 5  $\mu\text{L}$  Nafion diluent was dropped on the electrode in order to prevent dissolution. The synthesis route of CDs-ZnO/MWCNTs modified electrode was shown in **Fig. 1**. The CDs-ZnO composite was adhered to MWCNTs fabricated the CDs-ZnO/MWCNTs composite. There are lots of carboxyl groups on the surface of CDs and MWCNTs, and lots of hydroxyl group on the surface of ZnO. Therefore, they can connect to each other easily. The synthesis mechanism was further demonstrated by the FT-IR spectroscopy.

**Fig. 1**

## 3. Results and discussion

### 3.1 Characterization of CDs, CDs-ZnO, CDs-ZnO/MWCNTs

The morphologies of CDs, CDs-ZnO, CDs-ZnO/MWCNTs were shown in **Fig. 2(A-D)** by transmission electron microscope (TEM) and scanning electron microscope (SEM). The size of CDs was below 5 nm and the ZnO particles were nearly 50 nm. The CDs-ZnO/MWCNTs were interconnected with each other actually. In the enlarged TEM picture of CDs-ZnO/MWCNTs,



CDs-ZnO was stuck to MWCNTs. The X-ray diffraction (XRD) of CDs-ZnO and CDs-ZnO/MWCNTs were shown in **Fig. 3**, which further illustrated their compositions. The characteristic diffraction peaks of ZnO nanoparticles in XRD pattern corresponded to the typical Wurtzite ZnO phase (JCPDS 36-1451).<sup>37</sup> The XRD patterns of the CDs displayed a peak centered at 25.6° (002) in **Fig. 3A**.<sup>33,38,39</sup> The XRD patterns of the MWCNT showed a broad peak centered at 26.5° (002) in **Fig. 3B**.<sup>40</sup> The peak of CDs was affected by MWCNTs due to their nearly position.

**Fig. 2**

**Fig. 3**

The Fourier transform infrared spectroscopy (FT-IR) of CDs, ZnO, MWCNTs, CDs-ZnO, and CDs-ZnO/MWCNTs were shown in **Fig. 4**. The peaks of CDs at 3262 cm<sup>-1</sup> and 1646 cm<sup>-1</sup> corresponded to the stretching vibrations of O-H and C=O, respectively. The peaks at the range of 1000-1300 cm<sup>-1</sup> were attributed to the C-OH stretching and O-H bending vibrations.<sup>41, 42</sup> The peaks mentioned above implied the existence of large numbers of carboxyl groups in CDs aqueous systems. The peak at nearly 500 cm<sup>-1</sup> was contributed to the stretching of ZnO.<sup>43,44</sup> The peak of MWCNTs at 1699 cm<sup>-1</sup> was attributed to the stretching vibrations of C=O which could prove the successful acidification for MWCNTs. In the spectroscopy of CDs-ZnO, the sharp peaks at the range of 3400-3600 cm<sup>-1</sup> demonstrated the intermolecular association by hydrogen bonding between CDs and ZnO. The peaks at the range of 1620-1500 cm<sup>-1</sup> resulted from the C=O of -COOH and -COO- stretching vibration. Due to the interaction between them, especially the structure of MWCNTs for the conjugate system, the peak for the stretching vibrations of C=O was reduced to 1591 cm<sup>-1</sup> in the spectroscopy of CDs-ZnO/MWCNTs. The data showed that the

–COOH of CDs and MWCNTs had been formed the –COOZnOH when they were interacted with ZnO. And the FT-IR data confirmed the synthesis route of CDs-ZnO/MWCNTs.

**Fig. 4**

### 3.2 Cyclic voltammetric and electrochemical impedance spectroscopy response of CDs-ZnO/MWCNTs to HQ and CC

In **Fig.5A**, the electrochemical behaviors of bare GCE, Nafion/CDs, Nafion/CDs-ZnO, Nafion/ZnO/MWCNTs, Nafion/CDs-ZnO/MWCNTs were detected in 1.0 mM  $K_3[Fe(CN)_6]$  mixed solution contained 0.1 M KCl by cyclic voltammetry (CV). The electrode modified with CDs-ZnO/MWCNTs composite has the biggest redox peak current. By detecting the CV of the Nafion CDs-ZnO/MWCNTs/GCE in  $K_3[Fe(CN)_6]$  with different scan rate, the equation of linear regression between the peak current and the square root of the scan rate can be described by Randles-Sevcik's equation.<sup>45</sup>

$$I_{pa} = 2.69 \times 10^5 n^{3/2} A C_0 D \nu^{1/2}$$

In this equation,  $I_{pa}$  is the anodic peak current,  $n$  is the electron transfer number,  $A$  is the surface area of the electrode,  $D$  is the diffusion coefficient,  $C_0$  is the concentration of  $K_3[Fe(CN)_6]$ ,  $\nu$  is the scan rate. In 1.0 mM  $K_3[Fe(CN)_6]$  solution contained 0.1 M KCl,  $n=1$  and  $D=7.6 \mu\text{cm s}^{-1}$ . By the slope of the  $I_{pa} - \nu^{1/2}$  relationship, the surface area of bare GCE was found to be  $0.024 \text{ cm}^2$  and the CDs-ZnO/MWCNTs/GCE was calculated to be  $0.03 \text{ cm}^2$ , which increased nearly 1.25 times.

Electrochemical impedance spectroscopy (EIS) is further used for the investigation on the modified electrodes, which can exhibit the impedance changes of the modification processes. The value of the electrode-transfer resistance ( $R_{et}$ ) depends on the dielectric and insulating features at

the electrode/electrolyte interface. **Fig. 5B** showed the EIS of different electrodes in 1.0 mM  $[\text{Fe}(\text{CN})_6]^{3-/4-}$  and 0.1 M KCl solution. On the GCE the Ret value was got as 140  $\Omega$ . While on the Nafion/GCE the Ret value was decreased to 148  $\Omega$ . However, on the Nafion/CDs/GCE, the Ret value was decreased to 96  $\Omega$ , which could be attributed to the presence of high conductive CDs in the composite film that accelerated the electron transfer rate of  $[\text{Fe}(\text{CN})_6]^{3-/4-}$ . On the Nafion/CDs-ZnO/GCE, the Ret value was decreased to 57  $\Omega$ , indicated that the electrochemical performance of Nafion/CDs-ZnO was better than Nafion/CDs/GCE. The Ret value of Nafion/MWCNTs, Nafion/ZnO/MWCNTs and Nafion/CDs-ZnO/MWCNTs was 40  $\Omega$ , 34  $\Omega$  and 22  $\Omega$ , respectively. The results showed that the Nafion/CDs-ZnO/MWCNTs had best electrochemical performance. Hence, This was also strongly proved that Nafion/CDs-ZnO/MWCNTs could be a promising electrochemical platform for sensing.

### Fig.5

As shown in **Fig. 6**, the electrochemical behaviors of HQ and CC at different electrodes were investigated by cyclic voltammetry at 0.1 V s<sup>-1</sup> scan rate in 0.1 M PBS (pH = 4.5) contained 0.1 mM HQ and 0.1 mM CC. As shown in the inset of **Fig. 6**, there were only one peak of bare GCE, Nafion/GCE, Nafion/CDs/GCE and Nafion/CDs-ZnO/GCE. The Nafion had excellent film-forming. However, the peak current of Nafion/GCE was weakened significantly for their poorly electrical conductivity. After modifying the Nafion/CDs on the GCE, the electrochemical performance increased, and when dropping the Nafion/CDs-ZnO on the GCE, the electrochemical performance is better than the Nafion/CDs/GCE, which indicated the CDs and ZnO improve the electrochemical performance of this system. Both the different space resistances of HQ and CC and the fast electrochemical reaction kinetics of CDs-ZnO/MWCNTs contributed to the separation

of HQ and CC. The density of electron cloud of HQ molecule is higher than CC, leading to a decrease of oxidation activity at electrode surface for the latter.<sup>17, 41</sup> Different electron cloud density between HQ and CC lead to their different oxidized potential. Therefore, the voltammetric waves of HQ and CC could be separated.<sup>23,46,47</sup> The CDs-ZnO/MWCNTs modified electrode displayed the biggest electrochemical signals with two independently well-defined oxidation peaks at 0.207 V and 0.311 V of HQ and CC, respectively. The anodic potential difference ( $\Delta E_{pa}$ ) between HQ and CC of CDs-ZnO/MWCNTs was 0.104 V, which indicated the modified electrode could detect the HQ and CC simultaneously with high sensitivity.

**Fig. 6**

### 3.3 Effects of pH and scan rate

As shown in **Fig. 7**, the electrochemical behavior of HQ and CC was investigated by CV in PBS solution with pH range from 3.5 to 8.5. When the pH was 4.5, the oxidation current was maximized. Thus the pH value of 4.5 was chosen as the appropriate pH. As shown in **Fig. 7B**, as pH increased, the potentials of HQ and CC shifted negatively which indicated the proton was directly involved in the electrochemical redox process.<sup>27,48</sup> The linear regression equations between the potentials and pH of HQ and CC were  $E_{pa} \text{ (V)} = 0.453 - 0.052 \text{ pH}$  ( $R = 0.9927$ ) and  $E_{pa} \text{ (V)} = 0.534 - 0.049 \text{ pH}$  ( $R = 0.9920$ ) respectively. According to the mechanism of Nernst Equation ( $dE_p/dpH = 2.303 \text{ mRT}/nF$ ), the electrochemical redox of HQ and CC at the modified electrode should be a two electrons and two protons process.

The effects of scan rate was investigated in 0.1 M PBS (pH = 4.5) at CDs-ZnO/MWCNTs modified electrode from  $0.1 \text{ V s}^{-1}$  to  $0.5 \text{ V s}^{-1}$  by CV. As shown in **Fig. 8**, the redox peak currents increased gradually as the scan rate increased. The regression equations of HQ and CC were  $I_{pa}$

( $\mu\text{A}$ ) =  $54.743 - 7.706 v^{1/2}$  ( $\text{mV s}^{-1}$ ) ( $R = 0.9956$ ) and  $I_{\text{pa}}$  ( $\mu\text{A}$ ) =  $46.305 - 6.841 v^{1/2}$  ( $\text{mV s}^{-1}$ ) ( $R = 0.9954$ ) respectively. The peaks current was linearly associated with the square root of scan rate which indicated that the electrode reaction of HQ and CC at CDs-ZnO/MWCNTs /GCE was a typical diffusion-controlled process.

**Fig. 7**

**Fig. 8**

### 3.4 Simultaneous determination of HQ and CC

Differential pulse voltammetry (DPV) was chosen to study the simultaneous and quantitative determination of HQ and CC at CDs-ZnO/MWCNTs/GCE. Individual determination of HQ or CC was achieved in their mixed solution by changing the concentration of one species while keeping the other constant. **Fig. 9A** showed that increasing the concentration of HQ from 5.0 to 200  $\mu\text{M}$  while keeping the concentration of CC at 100  $\mu\text{M}$ , the peak current increased proportionally. Similarly, the peak current of CC increased as its concentration increased as shown in **Fig. 9B**. And the linear regression equation between the oxidation peak current and the concentration of HQ or CC showed a good linear relationship:  $I_{\text{pa(HQ)}} (\mu\text{A}) = -64.24 - 0.284 c (\mu\text{M})$  ( $R = 0.9950$ ) or  $I_{\text{pa(CC)}} (\mu\text{A}) = -44.15 - 0.385 c (\mu\text{M})$  ( $R = 0.9970$ ). The detection limit of HQ and CC was calculated to be 0.02  $\mu\text{M}$  and 0.04  $\mu\text{M}$  ( $S/N = 3$ ) respectively. The error bars of HQ and CC were below 1%. These experimental illustrated that the CDs-ZnO/MWCNTs modified electrode could improve the electrochemical currents and enhanced the catalytic separation performance.

**Fig. 9**

### 3.5 Interference effect

The influence of interferences for detection HQ and CC in real sample was necessary. The

interference substances were added in the 0.1 mM HQ and 0.1 mM CC mixture. The change of current caused by 1000-fold  $\text{Na}^+$ ,  $\text{K}^+$ ,  $\text{Mg}^{2+}$ ,  $\text{Cu}^{2+}$ ,  $\text{Zn}^{2+}$ ,  $\text{Cl}^-$ ,  $\text{SO}_4^{2-}$ ,  $\text{NO}_3^-$  and 0.1 mM resorcinol was less than 5%, which indicated the excellent selectivity and sensitivity of CDs-ZnO/MWCNTs modified electrode.

### 3.6 Sample analysis

The comparison of electrochemical analytical methods with different modified electrodes was shown in **Table 1**. In order to validate of the proposed method, the CDs-ZnO/MWCNTs electrode was applied to detect the HQ and CC in tap water. The standard solution was added to the tap water sample to obtain the recovery rate. The analytical results were displayed in **table 2** that the recovery rates of HQ and CC were 99.3%-105.4% and 104.3%-110.1% respectively. The recovery rates indicated that the CDs-ZnO/MWCNTs modified electrode has practical applicability and good accuracy in simultaneous determination of HQ and CC.

**Table 1**

**Table 2**

### 3.7 Stability and reproducibility

The stability and reproducibility of the CDs-ZnO/MWCNTs modified electrode were investigated by DPV contained 0.1 mM HQ and 0.1 mM CC by means of six time parallel determination. The relative standard deviation (RSD) of HQ and CC were 0.206 % and 0.176 % respectively. Therefore, the CDs-ZnO/MWCNTs electrode has excellent stability and reproducibility.

**Fig. 10**

#### 4. conclusions

In this work, CDs-ZnO/MWCNTs composite material was synthesized by a simple and convenient microwave synthesis with the help of Monowave 300. In summary, the CDs-ZnO/MWCNTs modified electrode was sensitive and selective for detecting the HQ and CC simultaneously. The peak currents of HQ and CC were well separated for more than 100 mV. The detection limits of HQ and CC were 0.02  $\mu\text{M}$ , 0.04  $\mu\text{M}$  ( $S/N = 3$ ) respectively. The CDs-ZnO/MWCNTs showed excellent stability and anti-interference ability. And the electrochemical method could be applied for simultaneous detection in real water sample.

#### Acknowledgements

This experiment was supported by the science and technology foundation of the national general administration of quality supervision in China (NO. 2012QK053), Fujian province natural science foundation (NO. 2012D136), the education bureau of Fujian province of China (NO. JA13195, JAT160875 and JAT160302), the natural science foundation of Zhangzhou (No. ZZ2016J31), the science and technology foundation of Fujian provincial bureau of quality and technical supervision (NO. FJQI2012029, NO. FJQI2013108) and the training programme foundation for excellent youth researching talents of Fujian's Universities (Fujian Education Section, 2016, No. 23).

## References

- 1 S. Zhu, W. Gao, L. Zhang, J. Zhao and G. Xu, *Actuat. B-Chem.*, 2014, **198**, 388-394.
- 2 T. C. Canevari, L. T. Arenas, R. Landers, R. Custodio and Y. Gushikem, *Analyst*, 2013, **138**, 315-324.
- 3 X. Li, G. Xu, X. Jiang and J. Tao, *J. Electrochem. Soc.*, 2014, **161**, H464-H468.
- 4 G. Zhao, M. Li, Z. Hu, H. Li and T. Cao, *J. Mol. Catal. A: Chem.*, 2006, **255**, 86-91.
- 5 X. Wang, M. Xi, M. Guo, F. Sheng, G. Xiao, S. Wu, S. Uchiyama and H. Matsuura, *Analyst*, 2016, **141**, 1077-1082.
- 6 S. C. Moldoveanu and M. Kiser, *J. Chromatogr. A*, 2007, **1141**, 90-97.
- 7 P. Nagaraja, R. A. Vasantha and K. R. Sunitha, *J. Pharmaceut. Biomed.*, 2001, **25**, 417-424.
- 8 H. Cui, C. He and G. Zhao, *J. Chromatogr. A*, 1999, **855**, 171-179.
- 9 A. Asan and I. Isildak, *J. Chromatogr. A*, 2013, **988**, 145-149.
- 10 M. F. Pistonesi, N. M. S. Di, M. E. Centurión, M. E. Palomeque, A. G. Lista and B. B. S. Fernández, *Talanta*, 2006, **69**, 1265-1268.
- 11 X. Yue, S. Pang, P. Han, C. Zhang, J. Wang and L. Zhang, *Electrochem. Commun.*, 2013, **34**, 356-359.
- 12 M. A. Ghanem, *Electrochem. Commun.*, 2007, **9**, 2501-2506.
- 13 J. Liu, M. D. Morris, F. C. Macazo, L. R. Schoukroun-Barnes and R. J. White, *J. Electrochem. Soc.*, 2014, **161**, H301-H313.
- 14 J. Liu, S. Wagan, M. D. Morris, J. Taylor and R. J. White, *Anal. Chem.*, 2014, **86**, 11417-11424.
- 15 T. Lai, W. Cai, W. Dai and J. Ye, *Electrochim. Acta*, 2014, **138**, 48-55.



- 16 X. Zhou, Z. He, Q. Lian, Z. Li, H. Jiang and X. Lu, *Sensor. Actuat. B-Chem.*, 2014, **193**, 198-204.
- 17 X. Feng, W. Gao, S. Zhou, H. Shi, H. Huang and W. Song, *Anal. Chim. Acta*, 2013, **805**, 36-44.
- 18 F. C. Moraes, M. F. Cabral, L. H. S. Mascaro and A. S. Machado, *Surf. Sci.*, 2011, **605**, 435-440.
- 19 A. T. Masheter, P. Abiman, G. G. Wildqoose, E. Wong, L. Xiao, N. V. Rees, R. Taylor, G. A. Attard, R. Baron, A. Crossley, J. H. Jones and R. G. Compton, *J. Mater. Chem.*, 2007, **17**, 2616-2626.
- 20 D. Yuan, S. Chen, R. Yuan, J. Zhang and W. Zhang, *Analyst*, 2013, **138**, 6001-6006.
- 21 W. Lian, S. Liu, J. Yu, J. Li, M. Cui, W. Xu and J. Huang, *Biosens. Bioelectron.*, 2013, **44**, 70-76.
- 22 Y. Quan, Z. Xue, H. Shi, X. Zhou, J. Du, X. Liu and X. Lu, *Analyst*, 2012, **137**, 944-952.
- 23 M. Tak, V. Gupta and M. Tomar, *J. Mater. Chem. B*, 2013, **1**, 6392-6401.
- 24 M. R. Shahmiri, A. Bahari, H. Karimi-maleh, R. Hosseinzadeh and N. Mirnia, *Sensor. Actuat. B-Chem.*, 2013, **177**, 70-77.
- 25 Y. Gao, Y. Cao, D. Yang, X. Luo, Y. Tang H. Li and J. Hazard. *Mater.*, 2012, **199-200**, 111-118.
- 26 Y. E. Shih and R. J. Jeng, *Oxford University Press Inc.*, New York, 2011, pp. 101-122.
- 27 F. Avilés, J. V. Gauich-Rodríguez, L. Moo-Tah, A. May-Pat and R. Vargas-Goronado, *Carbon*, 2009, **47**, 2970-2975.
- 28 Y. Li, S. Feng, S. Li, Y. Zhang and Y. Zhong, *Sensor. Actuat. B-Chem.*, 2014, **190**, 999-1005.
- 29 Q. Huang, X. Lin, F. Li, W. Weng, L. Lin and S. Hu, *Prog. Chem.*, 2015, **27**, 1604-1614.
- 30 Q. Huang, X. Lin, C. Lin, Y. Zhang, S. Hu, C. Wei, *RSC Adv.*, 2015, **5**, 54102-54108.

- 31 Y. Du and S. Guo, *Nanoscale*, 2016, **8**, 2532-2543
- 32 Q. Huang, H. Zhang, S. Hu, F. Li, W. Weng, J. Chen, Q. Wang, Y. He, W. Zhang and X. Bao, *Biosens. Bioelectron.*, 2014, **52**, 277-280.
- 33 A. Umar, M. M. Rahman, M. Vaseem and Y. B. Hahn, *Electrochem. Commun.*, 2009, **11**, 118-121.
- 34 J. Liu, C. Guo, C. M. Li, Y. Li, Q. Chi, X. Huang, L. Liao and T. Yu, *Electrochem. Commun.*, 2009, **11**, 202-205.
- 35 R. Ahmad, N. Tripathy, S. H. Kim, A. Umar, A. Al-Hajry and Y. Hahn, *Commun.*, 2014, **38**, 4-7.
- 36 M. Yu, D. Shao, F. Lu, X. Sun, H. Sun, T. Hu, G. Wang, S. Sawyer, H. Qiu and J. Lian, *Electrochem. Commun.*, 2013, **34**, 312-315.
- 37 H. Yu, H. Zhang, H. Huang, Y. Liu, H. Li, H. Ming and Z. Kang, *New J. Chem.*, 2012, **36**, 1031-1035.
- 38 D. Sun, R. Ban, P. Zhang, G. Wu, J. Zhang and J. Zhu, *Carbon*, 2013, **64**, 424-434.
- 39 Q. Huang, L. Zou, D. Chen, *RSC Adv.*, 2016, **6**, 82294-82297.
- 40 S. Banerjee and S. S. Wong, *J. Am. Chem. Soc.*, 2003, **125**, 10342-10350.
- 41 B. Chen, F. Li, S. Li, W. Weng, H. Guo, T. Guo, X. Zhang, Y. Chen, T. Huang, X. Hong, S. You, Y. Lin, K. Zeng and S. Chen, *Nanoscale*, 2013, **5**, 1967-1971.
- 42 M. L. Bhaisare, A. Talib, M. S. Khan, S. Pandey and H. Wu, *Microchimica. Acta*, 2015, **182**, 2173-2181.
- 43 F. Hassan, M. S. Miran, H. A. B. H. Susan and M. Y. A. Mollah, *Bangladesh J. Sci. Ind. Res.*, 2015, **50**, 21-28.

- 44 M. Tak, V. Gupta and M. Tomar, *J. Mater. Chem. B*, 2013, **1**, 6392-6401.
- 45 B. Rezaei and S. Damiri, *Sens. Actuators, B*, 2008, **134**, 324-331.
- 46 X. Feng, W. Gao, S. Zhou, H. Shi, H. Huang and W. Song, *Anal. Chim. Acta*, 2013, 805, 36-44.
- 47 D. W. Li, Y. T. Li, W. Song and Y. T. Long, *Anal. Methods-UK*, 2010, **2**, 837-843.
- 48 Z. Liu, Z. Wang, Y. Cao Y. Jing and Y. Liu, *Actuat. B-Chem.*, 2011, **157**, 540-546.
- 49 D. Song, J. Xia, F. Zhang, S. Bi, W. Xiang, Z. Wang, L. Xia, Y. Xia, Y. Li and L. Xia, *Actuat. B-Chem.*, 2015, **206**, 111-118.
- 50 S. Feng, Y. Zhang, Y. Zhong, Y. Li and S. Li, *J. Electroanal. Chem.*, 2014, **733**, 1-5.
- 51 A. T. E. Vilian, S. M. Chen, L. H. Huang, M. A. Ali and F. M. A. Al-Hemaid, *Electrochim. Acta*, 2014, **125**, 503-509.

### Tables

**Table 1.** Comparison of different electrochemical sensors for determination of HQ and CC.

**Table 2** The results of determination of HQ and CC in tap water samples.

**Table 1.** Comparison of different electrochemical sensors for determination of HQ and CC.

Electrode	Linear range ( $\mu\text{M}$ )		Detection limit ( $\mu\text{M}$ )		Ref.
	HQ	CC	HQ	CC	
N-GCE	5-260	5-260	0.2	0.2	4
MWCNTs-PDDA-GR	0.5-400	0.5-400	0.02	0.018	49
(CMWNTs-NHCH <sub>2</sub> CH <sub>2</sub> NH) <sub>6</sub> /GCE	10-120	5-80	2.3	1.0	50
Pt/ZrO <sub>2</sub> -RGO/GCE	1-1000	1-400	0.4	0.4	51
CDs-ZnO/MWCNTs	5-200	5-200	0.02	0.04	This work

**Table 2** The results of determination of HQ and CC in tap water samples.

samples	Added ( $\mu\text{L}$ )		Found ( $\mu\text{L}$ )		Recovery(%)		
	HQ	CC	HQ	CC	HQ	CC	
	1	20.0	20.0	18.2	23.2	99.3	102.4
Tap water	2	50.0	50.0	50.5	57.4	100.2	104.5
	3	80.0	80.0	72.8	76.5	97.6	98.2

### Figures

**Fig. 1.** The assemble mechanism of CDs-ZnO/MWCNTs.

**Fig. 2.** The TEM of CDs (A), CDs-ZnO (B), CDs-ZnO/MWCNTs (D) and the SEM of CDs-ZnO/MWCNTs (C) (insert: the enlarge TEM picture of CDs-ZnO/MWCNTs).

**Fig. 3.** The XRD pattern of CDs-ZnO (A) and CDs-ZnO/MWCNTs (B), inset were the XRD patterns of CDs and MWCNTs respectively.

**Fig. 4.** The Fourier transform infrared spectroscopy (FT-IR) of CDs, ZnO, MWCNTs, CDs-ZnO and CDs-ZnO/MWCNTs.

**Fig. 5.** CV (A) and EIS (B) of 1.0 mM  $K_3[Fe(CN)_6]$  recorded on the bare GCE, Nafion/GCE, Nafion/CDs, Nafion/CDs-ZnO, Nafion/MWCNTs, Nafion/ZnO/MWCNTs and Nafion/CDs-ZnO/MWCNTs.

**Fig. 6.** CV of 0.1 mM HQ and 0.1 mM CC recorded on bare GCE, Nafion/GCE, Nafion/CDs, Nafion/CDs-ZnO, Nafion/MWCNTs, Nafion/ZnO/MWCNTs and Nafion/CDs-ZnO/MWCNTs in the PBS (pH = 4.5) at the scan rate of 0.1 V s<sup>-1</sup>, inset was the CV of the bare GCE, Nafion/GCE, Nafion/CDs, Nafion/CDs-ZnO.

**Fig. 7.** (A) Effect of pH on the redox behavior of 0.1 mM and 0.1 mM CC in 0.1 M PBS at ZnO-CDs/MWCNTs (a-k: 3.5, 4.0, 4.5, 5.0, 5.5, 6.0, 6.5, 7.0, 8.0, 8.5) (B) plots of peak potential versus pH.

**Fig. 8.** (A) Effect of scan rate on the redox behavior of 0.1 mM HQ and 0.1 mM CC in 0.1 M PBS (pH =4.5) at CDs-ZnO/MWCNTs (a-i: 0.1, 0.15, 0.2, 0.25, 0.3, 0.35, 0.4, 0.45, 0.5 V s<sup>-1</sup>). (B) the square root of scan rate ( $v$ : 0.1-0.5 V s<sup>-1</sup>) for HQ and CC.

**Fig. 9.** DPVs of CDs-ZnO/MWCNTs (A) in the presence of 0.1 mM CC, containing different

concentrations of HQ (a-h: 5.0, 7.0, 10, 30, 50, 70, 100, 200  $\mu\text{mol L}^{-1}$ ), (B) in the presence of 0.1 mM HQ, containing different concentrations of CC (a-h: 5.0, 7.0, 10, 30, 50, 70, 100, 200  $\mu\text{mol L}^{-1}$ ), (C) was the calibration plots of HQ (a-h: 5.0, 7.0, 10, 30, 50, 70, 100, 200  $\mu\text{mol L}^{-1}$ ), (D) was the calibration plots of CC. (a-h: 5.0, 7.0, 10, 30, 50, 70, 100, 200  $\mu\text{mol L}^{-1}$ ).

**Fig. 10** The stability of repetitive measurements of DPV response for HQ (0.1 mM), CC (0.1 mM) in 0.1 M PBS (pH=4.5) at ZnO-CDs/MWCNTs modified electrode.



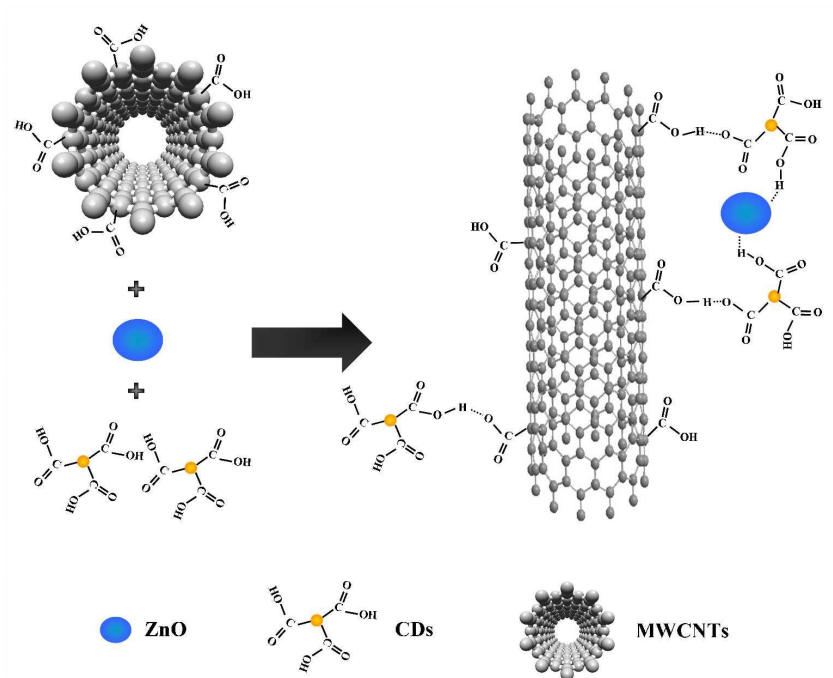


**Fig. 1.** The assemble mechanism of CDs-ZnO/MWCNTs.

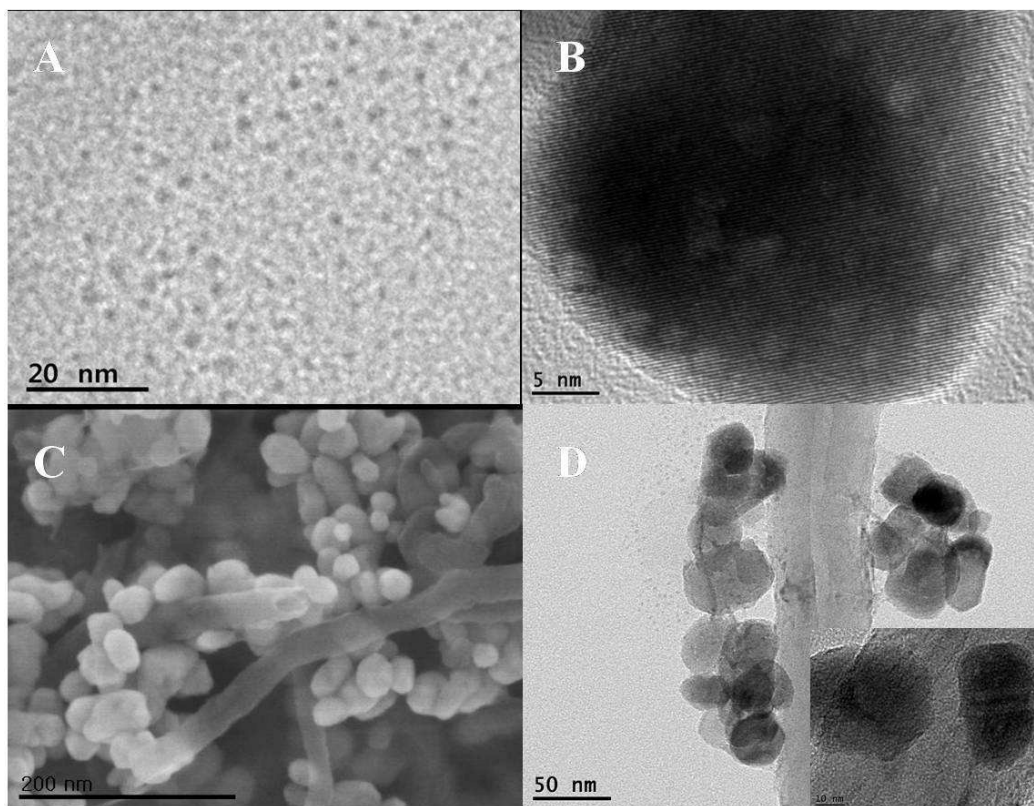


**Fig. 2.** The TEM of CDs (A), CDs-ZnO (B), CDs-ZnO/MWCNTs (D) and the SEM of CDs-ZnO/MWCNTs (C) (insert: the enlarge TEM picture of CDs-ZnO/MWCNTs).

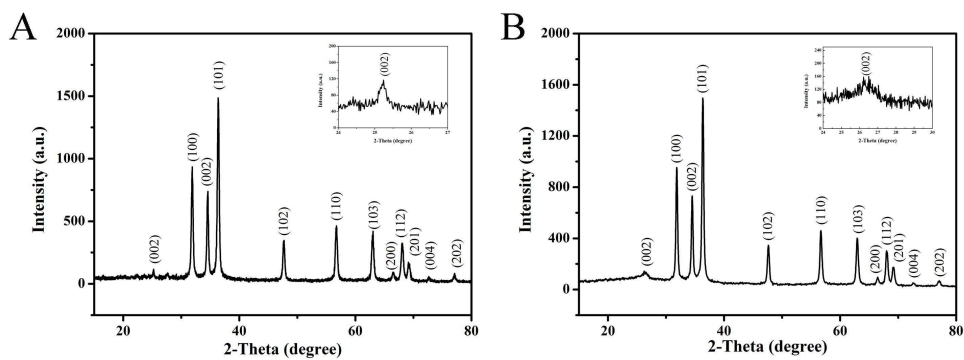


**Fig. 3.** The XRD pattern of CDs-ZnO (A) and CDs-ZnO/MWCNTs (B), inset were the XRD patterns of CDs and MWCNTs respectively.

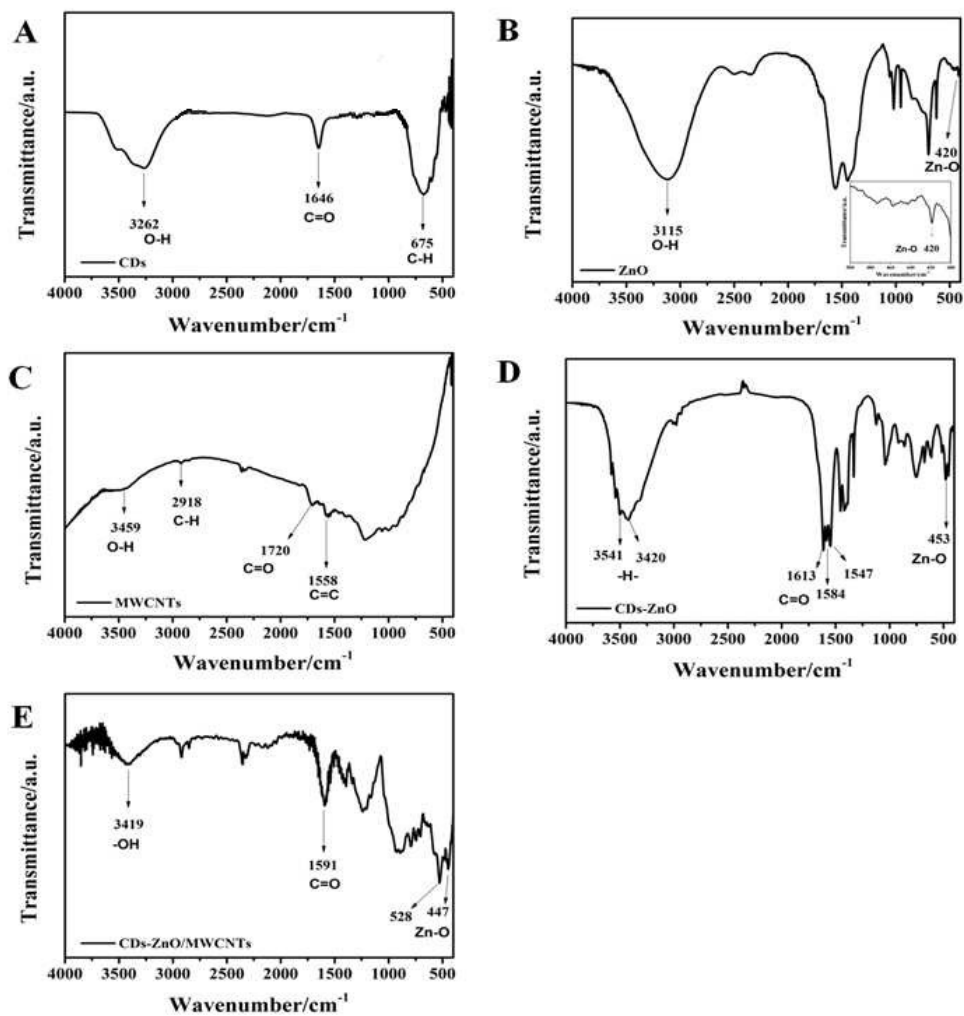


**Fig. 4.** The Fourier transform infrared spectroscopy (FT-IR) of CDs, ZnO, CDs-ZnO, MWCNTs and CDs-ZnO/MWCNTs.

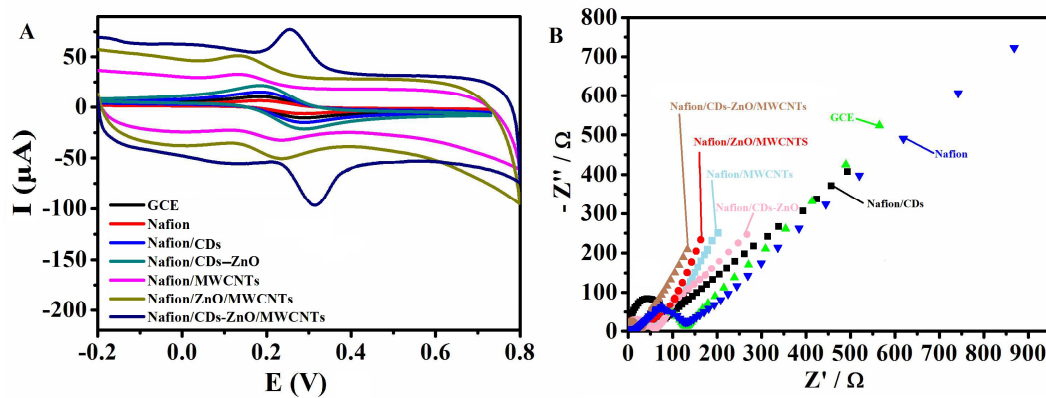
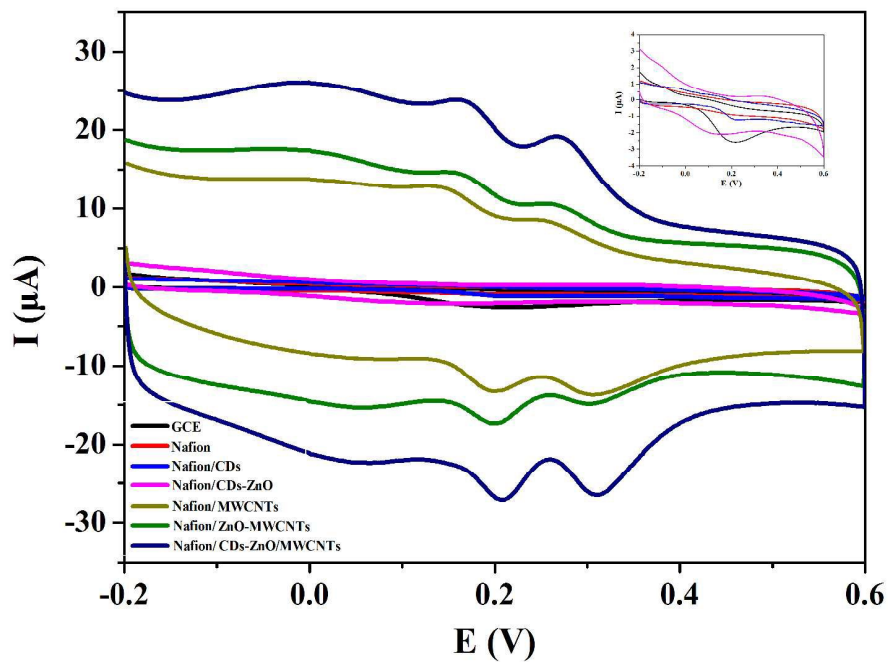


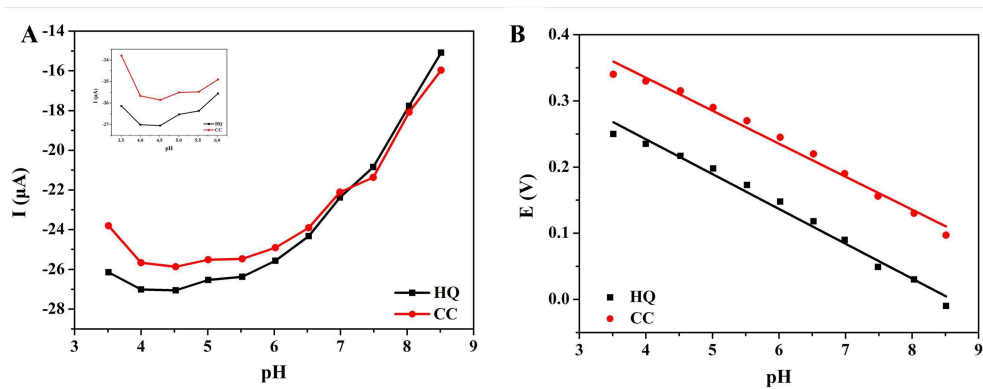
Fig. 5. CV (A) and EIS (B) of 1.0 mM  $\text{K}_3[\text{Fe}(\text{CN})_6]^{3-/4-}$  recorded on the bare GCE, Nafion/GCE,

Nafion/CDs, Nafion/CDs-ZnO, Nafion/MWCNTs, Nafion/ZnO/MWCNTs and

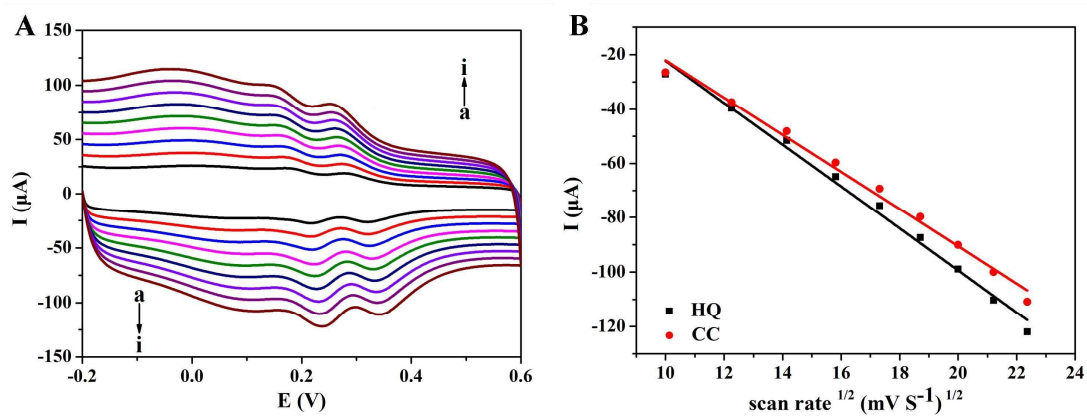
Nafion/CDs-ZnO/MWCNTs.



**Fig. 6.** CV of 0.1 mM HQ and 0.1 mM CC recorded on bare GCE, Nafion/GCE, Nafion/CDs, Nafion/CDs-ZnO, Nafion/MWCNTs, Nafion/ZnO/MWCNTs and Nafion/CDs-ZnO/MWCNTs in the PBS (pH = 4.5) at the scan rate of  $0.1 \text{ V s}^{-1}$ , inset was the CV of the bare GCE, Nafion/GCE, Nafion/CDs, Nafion/CDs-ZnO.

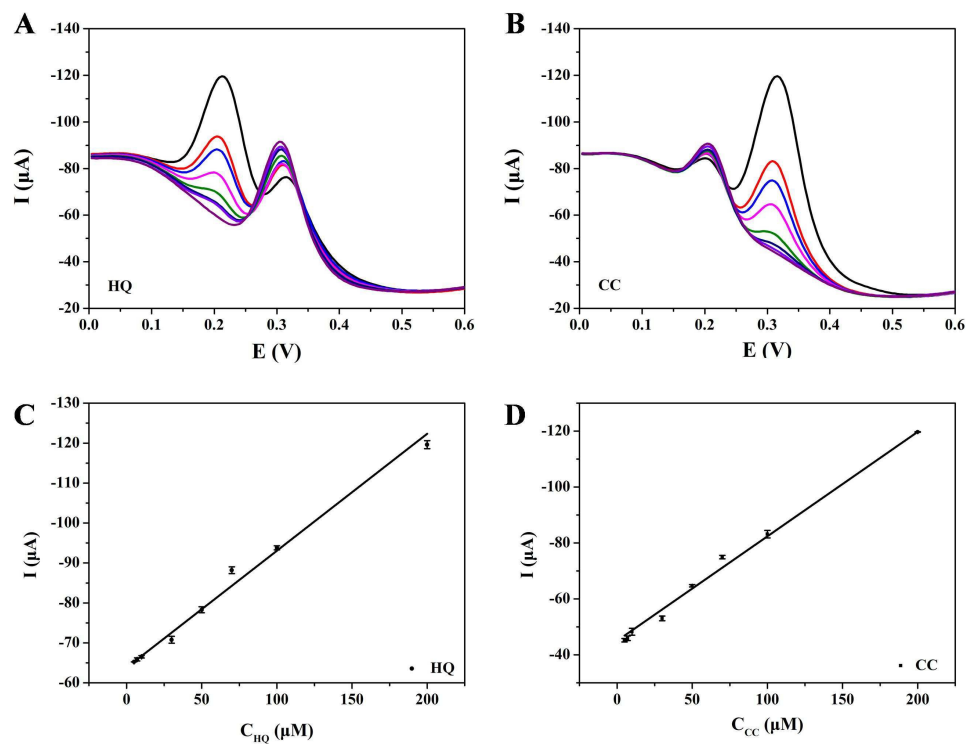


**Fig. 7.** (A) Effect of pH on the redox behavior of 0.1 mM HQ and 0.1 mM CC in 0.1 M PBS at ZnO-CDs/MWCNTs (a-k: 3.5, 4.0, 4.5, 5.0, 5.5, 6.0, 6.5, 7.0, 8.0, 8.5) (B) plots of peak potential versus pH.

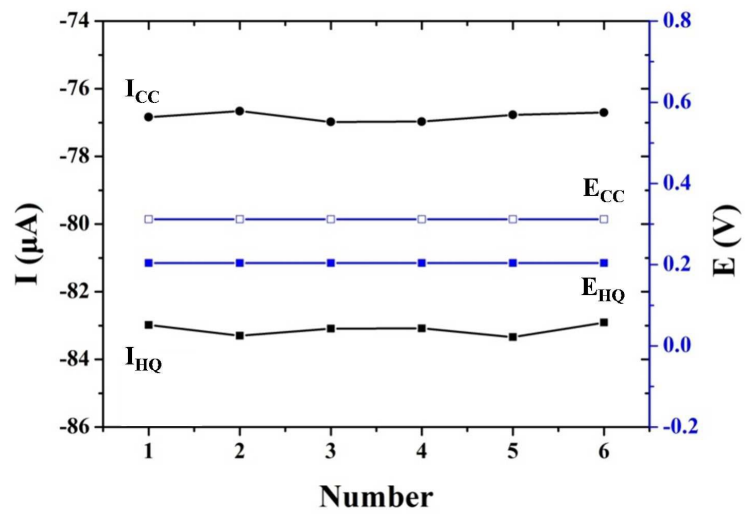


**Fig. 8.** (A) Effect of scan rate on the redox behavior of 0.1 mM HQ and 0.1 mM CC in 0.1 M PBS (pH =4.5) at CDs-ZnO/MWCNTs (a-i: 0.1, 0.15, 0.2, 0.25, 0.3, 0.35, 0.4, 0.45, 0.5 V s<sup>-1</sup>). (B) the square root of scan rate ( $v$ : 0.1-0.5 V s<sup>-1</sup>) for HQ and CC.



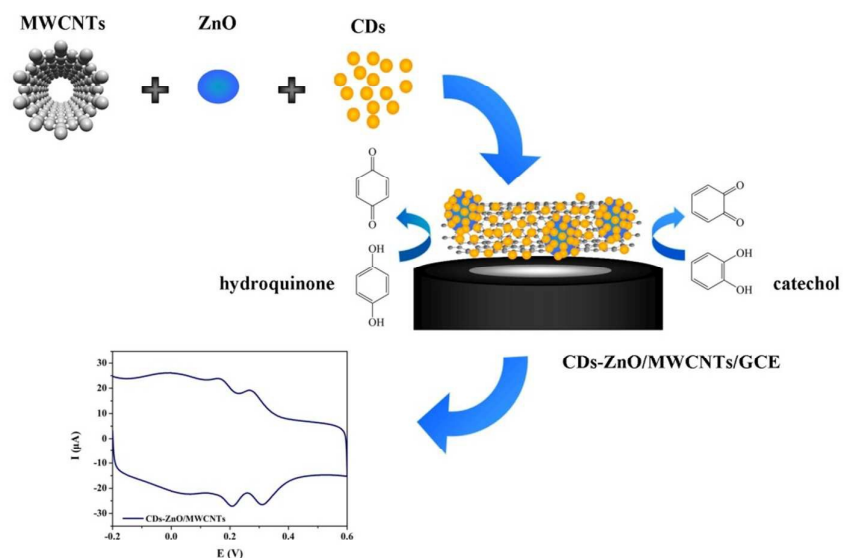


**Fig. 9.** DPVs of CDs-ZnO/MWCNTs (A) in the presence of 0.1 mM CC, containing different concentrations of HQ (a-h: 5.0, 7.0, 10, 30, 50, 70, 100, 200  $\mu\text{mol L}^{-1}$ ), (B) in the presence of 0.1 mM HQ, containing different concentrations of CC (a-h: 5.0, 7.0, 10, 30, 50, 70, 100, 200  $\mu\text{mol L}^{-1}$ ), (C) was the calibration plots of HQ (a-h: 5.0, 7.0, 10, 30, 50, 70, 100, 200  $\mu\text{mol L}^{-1}$ ), (D) was the calibration plots of CC. (a-h: 5.0, 7.0, 10, 30, 50, 70, 100, 200  $\mu\text{mol L}^{-1}$ ).



**Fig. 10.** The stability of repetitive measurements of DPV response for HQ (0.1 mM), CC (0.1 mM) in 0.1 M PBS (pH=4.5) at ZnO-CDs/MWCNTs modified electrode.

## Graphical Abstract



cyclic voltammety of HQ and CC recorded on Nafion/CDs-ZnO/MWCNTs/GCE